ISSN: 1231-4005
e-ISSN: 2354-0133
DOI: 10.5604/01.3001.0012.4340

IN-CYLINDER COMBUSTION ANALYSIS OF A SI ENGINE FUELLED WITH HYDROGEN ENRICHED COMPRESSED NATURAL GAS (HCNG): ENGINE PERFORMANCE, EFFICIENCY AND EMISSIONS

Romualdas Juknelevičius

Vilnius Gediminas Technical University
Faculty of Transport Engineering
J. Basanavičiaus Street 28, LT-03224 Vilnius, Lithuania
tel.: +370 5 2370583, fax: +370 5 2700112
e-mail: romualdas.juknelevicius@vgtu.lt

Roopesh Kumar Mehra, Fanhua Ma

Tsinghua University
State Key Laboratory of Automobile Safety and Energy
Beijing, 100084, People's Republic of China
tel.: +86 10 62785946, fax: +86 10 62785946
e-mail: luops15@mails.tsinghua.edu.cn
mafh@tsinghua.edu.cn

Stanislaw Szwaja

Czestochowa University of Technology
Faculty of Mechanical Engineering and Computer Science
Dabrowskiego Street 69, 42-201 Czestochowa, Poland
tel. +48 34 3250524, fax: +48 34 3250555
e-mail: szwaja@imc.pcz.czest.pl

Abstract

The main objective of this study was to investigate the effect of hydrogen addition on spark ignition (SI) engine's performance, thermal efficiency, and emission using variable composition hydrogen/CNG mixtures. The hydrogen was used in amounts of 0%, 20%, 40% by volume fraction at each engine speed and load. Experimental analysis was performed at engine speed of 1200 rpm, load of 120 Nm corresponding BMEP = 0.24 MPa, spark timing 26 CAD BTDC, and at engine speed of 2000 rpm, load of 350 Nm corresponding BMEP = 0.71 MPa, spark timing 22 CAD BTDC. The investigation results show that increasing amounts of hydrogen volume fraction contribute to shorten ignition delay time and decrease of the combustion duration, that also affect main combustion phase. The combustion duration analysis of mass fraction burned (MFB) was presented in the article. Decrease of CO_2 in the exhaust gases was observed with increase of hydrogen amounts to the engine. However, nitrogen oxides (NO_X) were found to increase with hydrogen addition if spark timing was not optimized according to hydrogen's higher burning speed.

Keywords: *Hydrogen, CNG, SI engine, combustion, emission, MFB*

1. Introduction

On March 28, 2011, the *White Paper* [1] was adopted in Brussels – the EC Transport Development Plan, which outlines the vision and implementation of a competitive and sustainable transport system of the EU. The *White Paper* sets the target for transport sector to reduce emissions by 60% and provides main objectives for the implementation of the competitive and efficient use of resources in the transport. Among these objectives are the targets by 2030 to

double-decrease the use of conventional fuel vehicles in cities, to achieve that vehicles in the major urban centres do not emit CO_2, while by 2050 to eliminate them out of cities at all [2].

Elimination of conventionally fuelled vehicles from the urban environment is a major contribution to significant reduction of oil dependence and greenhouse gas (GHG) emissions [1]. The *White Paper* states that for achievement of the highlighted objectives, there is no single fuel solution for the future transport as the availability and cost of alternative fuels differs between the modes and location. The benefits of alternative fuels are initially larger in urban areas with short travel distances where emissions are greater and options of various alternatives are available [2].

The compressed natural gas (CNG) is the alternative option most widely used in the market after LPG. The natural gas (NG) supplied not only by external suppliers but also obtained locally from biomass and waste biogas. It can fulfil a long-term perspective in terms of supply security and diversification of transport fuels [3]. Hydrogen is other alternative for transport as it is considered a perfect energy storage medium, and it can be produced either from fossil either non-fossil feedstocks [6-9]. However, high cost of hydrogen and lack of refuelling network makes it currently a rarely available and current use of hydrogen is limited to the role of a fuel additive [4]. As the NG vehicles (NGV) are a potential alternative with widely available fuelling network, the combustion of the hydrogen enriched CNG in spark ignition engines of NGV; enables further reduce the emissions [5].

The methane has a high octane number, enriched by hydrogen and supplied to the engine can operate on leaner air/fuel mixture which is more knock-resistant, and it enables for more flexible adjustments of engine operation parameters to improve the fuel economy [10]. It was found by several scientists, that hydrogen enriched CNG, increased the thermal efficiency of the engine, increased indicated mean effective pressure, and reduced fuel consumption [10-11, 13].

The enhancement of energy security and reduction of GHG emissions, gaseous fuels have been favoured by fast growing Chinese economy and automotive industry [9]. Because the performance of NG/CNG engines has some shortages at lean conditions, the concept to add the hydrogen as the additional fuel has been recognized by Chinese researchers, and series of researches on hydrogen – NG/CNG mixture fuelled engines have been carried out since the beginning of 2000 [5, 10, 13, 16-19]. Considering that plenty of research works have been done, this research is to conduct the effect of variable composition hydrogen enriched CNG mixtures (HCNG) on spark ignition engine's performance, emissions, ignition delay (lag) and combustion duration (expressed by CA0-10 and 10-90 of MFB).

2. Experimental device and test method

Tests performed at the State Key Laboratory of Automobile Safety and Energy, of Tsinghua University in Beijing, People's Republic of China. The in-line, six cylinder, Dongfeng model EQD210N-20 SI engine with turbocharger and intercooler has been used for the experiments at different operating conditions. The swept volume of the engine – 6234 cm^3, compression ratio – 10:1. The tests performed with the following hydrogen volume fractions: 0%, 20% and 40%. Manifold Absolute Pressure – MAP = 60-65 at engine speed of 1200 rpm, *BMEP* = 0.24 MPa and MAP = 135-137 MPa at engine speed of 2000 rpm, *BMEP* = 0.71 MPa. The spark timing was fixed 26º BTDC at *BMEP* = 0.24 MPa and at 22º BTDC at *BMEP* = 0.71 MPa.

The Eddy Current Dynamometer has used to measure and control the engine speed and load. The completely experimental installation presented at the Fig. 1. A high speed YOKOGAWA ScopeCorde was used to record the cylinder pressure data from a Kistler 6117B piezoelectric high-pressure transducer. Corresponding crankshaft positions are measured by a Kistler 2613B crank angle encoder with a resolution of 1º CA.

The exhaust concentration of NO_x, CO and CO_2 was measured by HORIBA-MEXA-7100DEGR emission monitoring system and the air/fuel ratio was measured by a HORIBA wide-range lambda analyser. An online hydrogen natural gas mixing system was developed to achieve

the desired amount of mixture, which is properly explained in Fig. 2. The pressure stabilizing HCNG tank was separated into two chambers with a damping line used to uplift the blend uniformity [21]. The flow rate of CNG and H_2 was measured by a Micro Motion flow meter that uses the principle of Coriolis force for a direct measure of mass flow. An ALICAT flow control valve was used to adjust the flow rate of the hydrogen according to the flow rate of CNG and obtain the target hydrogen fraction.

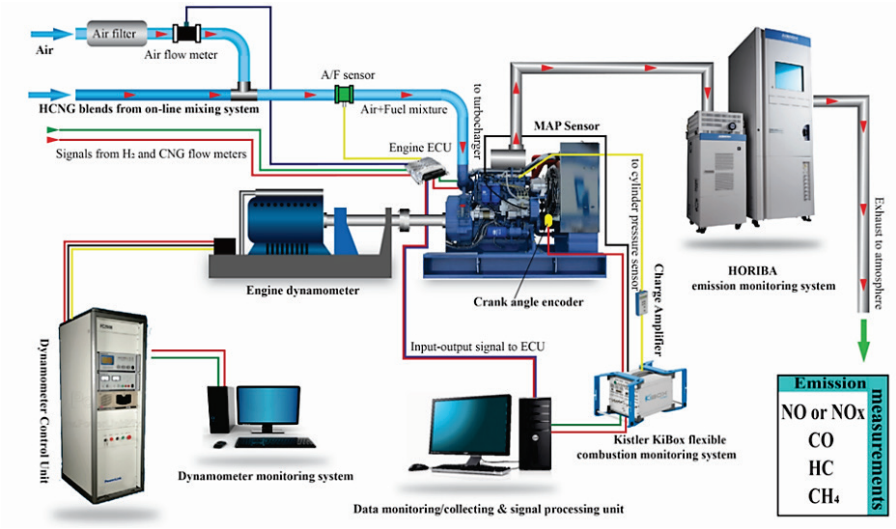

Fig. 1. Experimental set-up

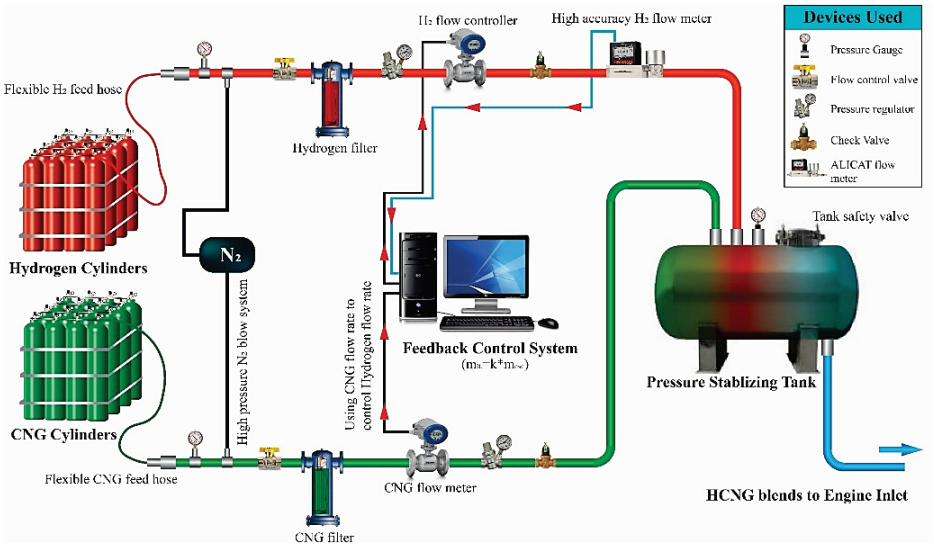

Fig. 2. High accuracy on-line HCNG blends preparation system (China Patent number ZL00710175797.9)

This system has been validated for varied hydrogen fractions with the test outcomes, and the comparison shows that the fuel mixing system performs well under all the conditions where the absolute error in hydrogen fraction is found always less than 1.5% [22]. The air mass flow rate is acquired by the thermal type gas mass flowmeter Toceil 20N100114LI.

The main fuel properties of the HCNG mixtures with 20%, and 40% hydrogen enrichment presented at the Tab. 2. The volumetric lower heating value with increase of hydrogen energy share (HES) of HCNG mixture decrease. The heating value of CNG+H20 is by 26.6% less in compare to CNG, while CNG+H40 are by 43.1% less than CNG. However, the LHV of a stoichiometric mixture is less influenced by the hydrogen enrichment; it differs in compare to the neat CNG by 5.2-8.4%.

Tab. 2. Properties of the HCNG (hydrogen-enriched natural gas) blends tested during the experiment

Properties	CNG	CNG+H20	CNG+H40
	n = 1200 rpm, *BMEP* = 0.24 MPa		
H_2 volume fraction, %vol	–	20	40
Air-fuel mixture equivalence ratio, λ (calculated)	1.043	1.129	1.071
LHV, MJ/kg	50.02	52.29	55.62
LHV, MJ/Nm^3	35.80	26.28	20.36
AFR_{vol} of stoichiometric mixture (λ = 1)	9.30	6.76	5.18
LHV_{vol} of stoichiometric mixture (λ = 1), MJ/Nm^3	3.47	3.29	3.18
	n = 2000 rpm, *BMEP* = 0.71 MPa		
H_2 volume fraction, %vol	–	20	40
Air-fuel mixture equivalence ratio, λ (calculated)	1.138	1.161	1.117
LHV, MJ/kg	50.02	52.15	55.38
LHV, MJ/Nm^3	35.8	26.57	20.63
AFR_{vol} of stoichiometric mixture (λ = 1)	9.30	6.84	5.25
LHV_{vol} of stoichiometric mixture (λ = 1), MJ/Nm^3	3.47	3.30	3.19

5. Test results and discussion

The main topic of the presented research was the impact of HES on combustion properties and combustion duration of the SI engine operating with the HCNG mixture at two engine speeds corresponding two *BMEP*: 1200 rpm at *BMEP* = 0.24 MPa and 2000 rpm at *BMEP* = 0.71 MPa. The spark timing was fixed at 26º BTDC with *BMEP* = 0.24 MPa and at 22º BTDC with *BMEP* = 0.71 MPa.

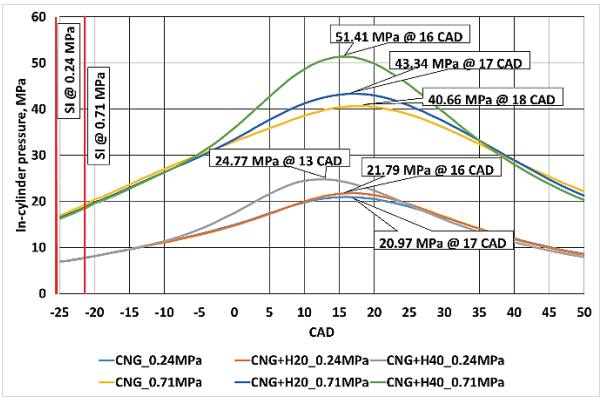

Fig. 3. The dependence of in-cylinder pressure on BMEP, engine speed and hydrogen fraction

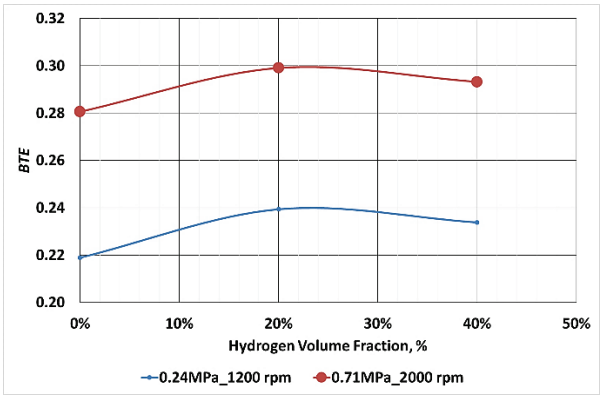

Fig. 4. The dependence of BTE on BMEP, engine speed and hydrogen fractions

In-cylinder pressure curves with maximum pressure (p_{max}) spark ignition (SI) timing for various hydrogen volume fractions provided at the Fig. 3. Maximum pressure data variations can be observed with the various hydrogen fractions and engine loads. The in-cylinder maximum pressure increased with increment of HES from 20.97 MPa with *BMEP* of 0.24 MPa (at 17 CAD ATDC), to 21.79 MPa during test of CNG+H20 and 24.77 MPa at 13 CAD ATDC in case of CNG+H40. At the higher *BMEP* of 0.74 MPa, the p_{max} was at 40.36 MPa with sole CNG and increased to 43.34 MPa (at 17 CAD ATDC) with CNG+H20, and up-to 51.41 MPa with CNG+H40. p_{max} raised with the increase of hydrogen fractions due to enhanced burning velocity, and quickly elevated pressure [5]. The trends of pressure-rise are nearly the same as the in-cylinder pressure.

As it can be seen at the Fig. 4 that the Brake Thermal Efficiency (*BTE*) reaches the peak of 0.3 with hydrogen volume fraction of 20% and then falls down with increase of hydrogen fraction to 40-vol%. It can be explained that presence of hydrogen with 20-vol% was helpful to realize complete combustion because of leaner gas mixture [10]. It was defined $\lambda = 1.129$ with CNG+H20, while with sole CNG $\lambda = 1.043$ and $\lambda = 1.071$ with CNG+H40 at 0.24 MPa of *BMEP*. The same phenomena were at 0.71 MPa. The combustion gets very unstable when the excess air ratio is close to the lean limit and the *BTE* was lower by 7-8% with sole CNG, while only by 2-3% with CNG+H40.

Figure 5 shows the CO and CO_2 emission versus hydrogen volume fraction. The CO emission mainly results from incomplete combustion and cracking of CO_2 at the high temperature [10]. With increase of hydrogen fraction, the temperature increased and effected increment of CO. The marginal increase of CO emission by 13-15% with CNG+H20 was mainly because the sufficient oxygen concentration with increased λ from 1.043 to 1.129. The further sharp gain of CO was the result of the increased temperature environment caused by hydrogen. The CO emission probably could increase due to the reduced flame quenching distance influenced by presence of hydrogen too [11].

The CO_2 emission data show (Fig. 5) that due to the H_2 co-combustion with CNG fuel it was possible to achieve lower CO_2 level because of less carbon in the gas mixture and increase of H/C atom ratio from 4 with sole CNG, to 5.2 with CNG+H40.

The NO_x emission increased with the increase of hydrogen fraction (Fig. 6). The NO_x emission was lower at 0.71 MPa of *BMEP* than that at 0.24 MPa when test was performed with sole CNG. Although the oxygen concentration at the 0.71 MPa of *BMEP* was higher ($\lambda = 1.138$) than at the 0.24 MPa ($\lambda = 1.043$). It means that due to the higher engine speed there was not enough time to emerge NO_x emission. Other reason could be the combustion temperature was lower which resulted in less NO_x formation. With increment of the hydrogen fraction and with increase of λ to 1.129 at *BMEP* = 0.24 MPa, and up-to 1.161 at *BMEP* = 0.71 MPa, increased the flame temperature at the both *BMEP*. With hydrogen fraction of 20% the NO_x raised to 230 ppm for *BMEP* of 0.24 MPa and 0.71 MPa. Further rise of NO_x was mainly affected by increment of hydrogen-influenced increase of the temperature.

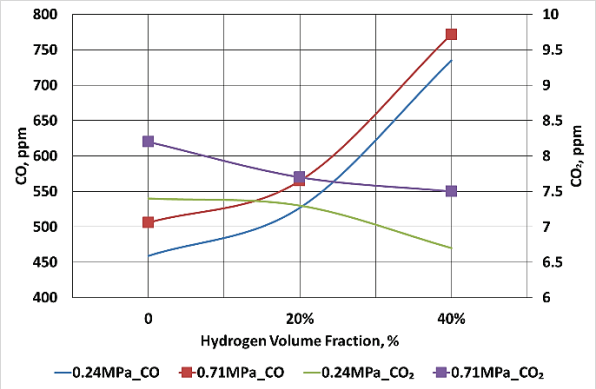

Fig. 5. The dependence of CO and CO_2 on BMEP, engine speed and hydrogen fractions

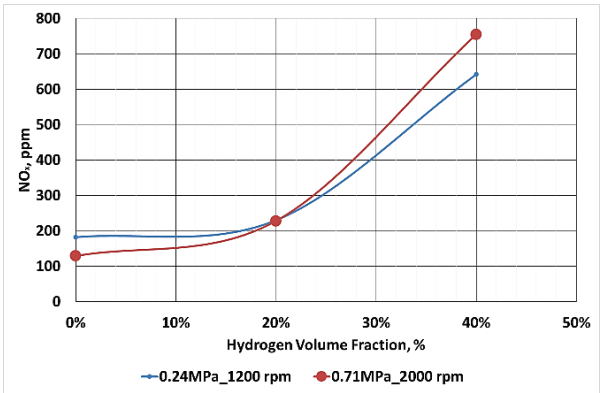

Fig. 6. The dependence of NO_x on BMEP, engine speed and hydrogen fractions

As illustrated in Fig. 7-8 the MFB was advanced with increment of hydrogen fraction. The MFB was calculated as the normalized cumulative heat release by the Rassweiler and Withrow method [12]. The combustion duration (CD) of CA0–10 is defined as the CA interval from the start of combustion to the CA of 10% MFB, while CD of CA10–90 is defined as the CA interval from the 10% MFB to the CA of 90% MFB. The combustion duration of CA0-10 and CA10-90 was calculated at each *BMEP* and with each hydrogen fraction for HCNG according to the MFB profiles.

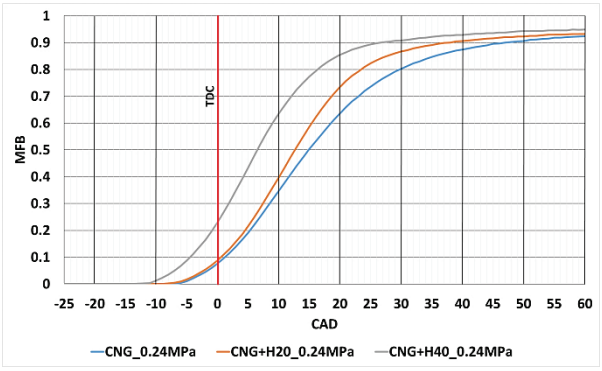

Fig. 7. The dependence of MFB on hydrogen fraction at the BMEP = 0.24 MPa and engine speed of 1200 rpm

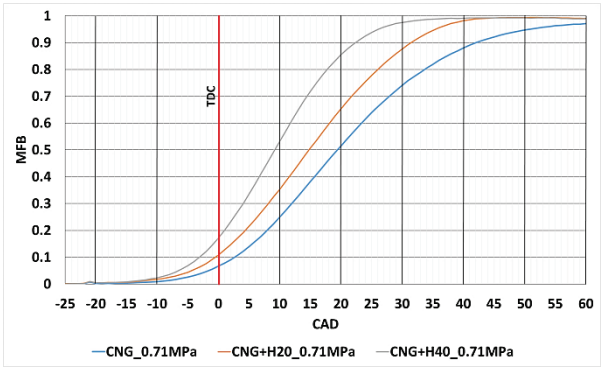

Fig. 8. The dependence of MFB on hydrogen fraction at the BMEP = 0.71 MPa and engine speed of 2000 rpm

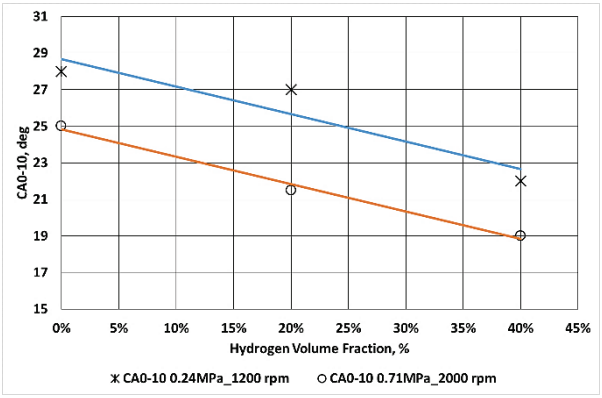

Fig. 9. The combustion duration of 0-10 MFB at the various hydrogen fractions, BMEP and engine speed

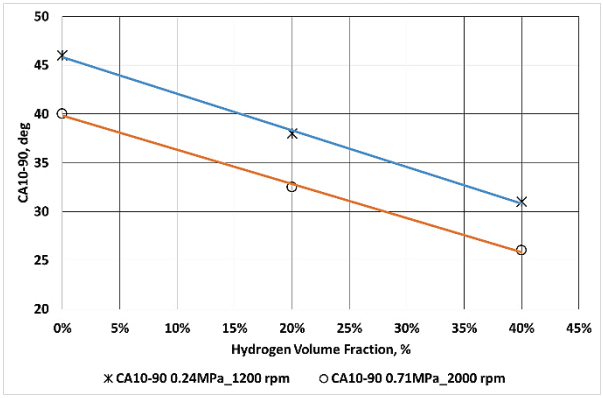

Fig. 10. The combustion duration of 10-90 MFB at the various hydrogen fractions, BMEP and engine speed

The increase of HES shortens the ignition delay (lag) expressed by the initial combustion duration of CA0-10 (Fig. 9) due to the high premixed combustion rate and development of higher laminar speed of hydrogen flame. Increase of hydrogen fraction also reduces the main combustion duration CA10-90 (Fig. 10) which was accelerated by the first combustion phase CA0-10 [13-14].

The hydrogen fraction supports the formation of very active H and OH radicals during the combustion, whose increase makes the combustion reaction much easier and faster, thus leading to the shorter CD [13–15, 20]. The additional H and OH radicals brought by the hydrogen addition increases the mixture's laminar flame speed, which during combustion of gaseous fuels has an effect on flame growth rate and it not becomes turbulent [14].

As it can be seen in the Fig. 7-10, the increase of hydrogen fraction shortens the ignition delay and moves the location of the 50% MFB closer to the TDC (Fig. 11). The most effective combustion of hydrogen – gas mixtures can be achieved when the highest value of the max. rate of MFB ($dMFB_{max}/d\phi$) is located just after the middle combustion phase (expressed by the 50% MFB), while it position within the range of 8-13 CAD is most favourable for internal combustion engines [14].

The $dMFB_{max}/d\phi$ vs. location of the 50% MFB is plotted at the Fig. 12. It can be seen the linear relation in between locations of the 50% MFB and the max. rate of MFB. The locations of the 50% MFB with 0.24 MPa of *BMEP* is closer to the TDC and better fit into the range of 8-13 CAD than that of 0.71 MPa of *BMEP*, because the earlier spark timing: 26 CAD BTDC at 0.24 MPa of *BMEP* in compare to 22 CAD BTDC of 0.71 MPa of *BMEP*.

6. Conclusions

The following main conclusions can be drawn from this study:

- the increase of p_{max} noticed with increase of hydrogen fraction due to enhanced burning velocity, and quickly elevated pressure,
- the hydrogen volume fraction of 20% was the most suitable with respect to the highest *BTE* noticed during the tests, while it falls down with increase of hydrogen fraction to 40 vol%,
- the marginal increase of CO and NO_x emissions noticed with CNG+H20 followed by significant increase with CNG+H40. However, the CO_2 emission decreased steadily with increase of hydrogen fraction,
- hydrogen volume fraction of 20% found as optimal percentage with respect to *BTE* and overall toxic emissions,
- hydrogen addition influences combustion phases: main combustion phase and ignition delay time. As observed, the ignition delay expressed by CA0-10 was shortened by 6 CAD. The CA10-90 was shorter with increase of hydrogen fraction as well,
- increase of hydrogen fraction move the position of the 50% MFB closer to TDC and increase the $dMFB_{max}/d\phi$. The spark timing and addition of hydrogen could be use as the tools for adjustment of desirable position of $dMFB_{max}/d\phi$ and it location in relation to the 50% MFB,
- the engine lean burn capability could be improved through hydrogen enrichment and this positive effect becomes increasingly more obvious as hydrogen enhancement level increases. The test results show that HCNG could be used for the enhancement of the SI engine.

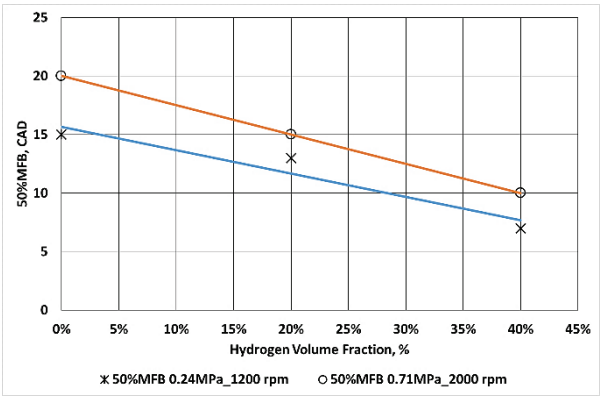

Fig. 11. The position of 50% MFB at the various hydrogen fractions, BMEP and engine speed

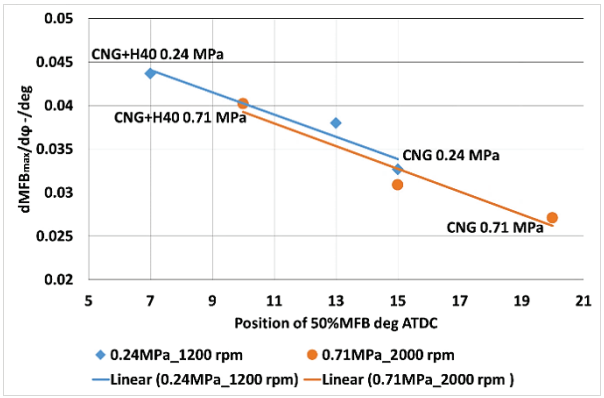

Fig. 12. The maximum rate of MFB $dMFB_{max}/d\phi$ as function of the 50% MFB position

Acknowledgments

Author wants to acknowledge and express his gratitude towards all the members of the research groups at Tsinghua University in Beijing, People's Republic of China and Czestochowa University of Technology in Poland for their advice, and support for the preparation of the manuscript.

References

[1] European Commision, *White Paper. Roadmap to a Single European Transport Area – Towards a competitive and resource efficient transport system*, Brussels 2011.
[2] European Commision, *Transport 2050*, Brussels 2011.
[3] European Commision, *Communication from the Commission to the European Parliament, The Council, The European Economic and Social Committee and the Committee of the Regions.* Clean Power for Transport: A European alternative fuels strategy, Brussels 2013.
[4] Bauer, C. G., Forest, T. W., et al., *Effect of hydrogen addition on performance of methane-fueled vehicles. Part I: Effect on SI engine performance*, Int J Hydrogen Energy, Vol. 26, pp. 55-70, 2001.

[5] Ma, F., Liu, H., Wang, Y., Li, Y., Wang, J., Zhao, S., *Combustion and emission characteristics of a port-injection HCNG engine under various ignition timings*, Int Journal of Hydrogen Energy, Vol. 33, pp. 816-822, 2008.
[6] Mehra, R. K., Duan, H., Juknelevičius, R., Ma, F., Li, J., *Progress in hydrogen enriched compressed natural gas (HCNG) internal combustion engines – A comprehensive review*, Renewable and Sustainable Energy Reviews, Vol. 80, pp. 1458-1498, 2017.
[7] Woodrow, W. C, Jeremy, R., *Hydrogen energy stations: along the roadside to the hydrogen economy*, Utilities Policy, Vol. 13, pp. 41-50, 2005.
[8] Billur, S., Farida, L. D., Michael, H., *Metal hydride materials for solid hydrogen storage: a review*, Int J Hydrogen Energy, Vol. 32, pp. 1121-1140, 2007.
[9] Sun, Z. Y., Liu, F. S., Liu, X. H., *Research and development of hydrogen fuelled engines in China*, Int J Hydrogen Energy, Vol. 37, pp. 664-681, 2012.
[10] Zhao, J., Ma, F., Xiong, X., Deng, X., Wang, L., Naeve, N., Zhao, S., *Effects of compression ratio on the combustion and emission of a hydrogen enriched natural gas engine under different excess air ratio*, Energy, Vol. 59, pp. 658-665, 2013.
[11] Melaika, M., *Research of a combustion process in a spark ignition engine, fuelled with gaseous fuel mixtures*, Doctoral dissertation, ISBN 978-609-457-996-7, Vilnius 2016.
[12] Rasswieler, G. M., Withrow, L., *Motion pictures of engine flames correlated with pressure cards*, SAE Paper No. 800131, 1980.
[13] Ma, F., Wang, M., Jiang, L., Chen, R., Deng, J., Naeve, N., Zhao, S., *Performance and emission characteristics of a turbocharged CNG engine fueled by hydrogen-enriched compressed natural gas with high hydrogen ratio*, International Journal of Hydrogen Energy, Vol. 35, pp. 6438-6447, 2010.
[14] Szwaja, S., *Knock and combustion rate interaction in a hydrogen fuelled combustion engine*, Journal of KONES Powertrain and Transport, Vol. 18, No. 3, pp. 431-438, 2011.
[15] Conte, E., Boulouchos, K., *Influence of hydrogen-rich-gas addition on combustion, pollutant formation and efficiency of an IC-SI engine*, SAE Paper No. 2004-01-0972, 2004.
[16] Miao, H. Y., Lu., L., Huang, Z.H., *Flammability limits of hydrogenenriched natural gas*, International Journal of Hydrogen Energy, Vol. 36, pp. 6937-6947, 2011.
[17] Ma, F., He, Y. T., Deng, J., Jiang, L., Naeve, N., Wang, M. Y., et al., *Idle characteristics of a hydrogen fueled SI engine*, International Journal of Hydrogen Energy, Vol. 36, Iss. 7, pp. 4454-4460, 2001.
[18] Ma, F., Wang, M. Y., Jiang, L., Deng, J., Chen, R. Z., Naeve, N., et al., *Performance and emission characteristics of a turbocharged spark-ignition hydrogen-enriched compressed natural gas engine under wide open throttle opening conditions*, International Journal of Hydrogen Energy, Vol. 35, Iss. 22, pp. 12502-12509, 2010.
[19] Ma, F., Li, S., Zhao, J., Qi, Z., Deng, J., Naeve, N., et al., *Effect of compression ratio and spark timing on the power performance and combustion characteristics of an HCNG engine*. Int J Hydrogen Energy, Vol. 37, pp. 18486-18491, 2012.
[20] Heywood, J. B., *Internal combustion engines fundamentals*, McGraw Hill Inc., p. 930, 1988.
[21] Yin, C. Q., Cheng, P., Gao, Y. H., Xing, S. H., *Study on property of a stable pressure box with damping line for engine experiment*, Nat Sci J Jilin Univ Technol, Vol. 31, pp. 75-78, 2001.
[22] Ma, F., Wang, Y., Wang, J., Zhao, S., Yin, Y., Cheng, W., et al., *Development and validation of an on-line hydrogen-natural gas mixing system for internal combustion engine testing*, SAE Technical Paper, 2008.

Manuscript received 09 May 2018; approved for printing 31 August 2018